Characterizing the gastrointestinal development and digestive enzyme ontogeny of larval *Amphiprion ocellaris*

Casey A. Murray[1]*, Olivia I. Markham[1], Sarah W. Hutchins[1], Matthew A. DiMaggio[1]

[1]University of Florida, Institute of Food and Agricultural Sciences, School of Forest, Fisheries, and Geomatics Sciences, Program in Fisheries and Aquatic Sciences, Tropical Aquaculture Laboratory

1408 24th Street SE, Ruskin, FL 33570

*corresponding author's email**: casey.murray@ufl.edu**

Abstract

Clownfish (*Amphiprion ocellaris*) are the most recognizable and popular marine aquarium fish and are a key commodity for marine ornamental fish producers. Although these fish have been raised in captivity for decades, producers are still experiencing issues regarding larval survival, reliance on live feeds, and post-larval deformities. To improve the culture process, the ontogeny of larval development and digestive capacity should be elucidated. The morphological development, digestive enzyme ontogeny, and digestive tract development of *A. ocellaris* was examined in a 16-day trial. Standard microplate assays were conducted to quantify the activity of trypsin, lipase, and acid protease enzymes from 24 hours before hatching to 15 days post hatch (DPH). Histology was used to visualize morphological changes in the digestive tract throughout the larval period. At hatching, *A. ocellaris* has functional eyes, an open mouth, and a coiled, differentiated digestive tract. Trypsin and lipase activities were detectable before hatching and increased significantly later in the larval period. Gastric gland formation was observed at 6 DPH, with stomach functionality occurring between 7 – 9 DPH, indicated by

gastric gland proliferation and an increase in acid protease activity. The results from this study may be used to inform weaning protocols to maximize larval growth and survival while minimizing the use of costly live feeds.

Keywords: clownfish, ornamentals, digestive enzymes, larviculture

1. Introduction

The international aquarium trade has been supplying home and public aquariums with ornamental fishes and invertebrates for several decades. The value of the industry is estimated at 15 – 30 billion USD, where marine fish and invertebrates account for nearly 300 million USD (Palmtag, 2017; Penning et al., 2009). Approximately 5,300 freshwater ornamental fish species and 2,500 marine ornamental fish species are traded worldwide (Raghavan et al., 2013; Rhyne et al., 2017). However, of the thousands of freshwater ornamentals exported, 90% are produced via aquaculture while most marine ornamentals still originate from wild stocks (Whittington and Chong, 2007). To improve the sustainability of the marine aquarium trade, the supply of marine ornamentals can be augmented with increased focus on aquaculture production of marine ornamental fishes.

Clownfishes of the family Pomacentridae are among the most popular and recognizable of marine ornamental fishes. Pomacentrids account for over 50% of the marine ornamental fish imported into the US by volume (Rhyne et al., 2012; Rhyne et al., 2017). Made globally popular by the 2003 film *Finding Nemo,* clownfishes, including *Amphiprion ocellaris* and *Amphiprion percula* were the fifth most imported marine ornamental fish into the US in 2004-2005 with

45 approximately 450,000 individuals imported (Rhyne et al., 2012). Displaying clownfishes in
46 aquaria dates to the 1960s, making them one of the first marine ornamentals to be traded
47 commercially (Palmtag, 2017). These fish were also the first marine ornamental fish to be
48 successfully cultured in 1974 (Hoff, 1996). In the decades since, over 15 species of clownfish
49 have been commercially produced and include many different color variations and several
50 hybrid species. Of the almost 30 'designer' *A. ocellaris* produced, individual fish can retail
51 anywhere from $20 USD to $280 USD (LiveAquaria.com, 2022), with prices based primarily on
52 unique coloration or body conformation. Clownfish have also become important model
53 organisms for studies on climate change, ocean acidification, ecotoxicology and ecology, as well
54 as developmental, and evolutionary biology (eco/evo/devo; Roux et al., 2019; Roux et al.,
55 2020). Several characteristics of clownfish, including their unique relationship with their host
56 anemone, endemism to coral reefs, and relative ease of culture in captivity facilitates the use of
57 these fish in both *in situ* and *ex situ* experiments.
58 While clownfishes have been cultured for several decades, scientific literature on basic
59 culture parameters, especially for *A. ocellaris*, is still incomplete. Although a few culture
60 manuals exist for *A. ocellaris* and *A. percula*, most of the data has not been empirically validated
61 and there are several instances of conflicting information among manuals (Ajith Kumar and
62 Balasubramanian, 2009; Hoff, 1996; Madhu et al., 2006; Roux et al., 2021). Commercial
63 clownfish producers have expressed concern over highly variable hatch success and larval
64 survival, heavy reliance on live feeds such as rotifers and *Artemia* sp., and the presence of
65 several different types of deformities in juvenile fish (Personal communication). These issues
66 lead to profit losses via reduced numbers of settled, sellable juveniles. Further investigations

into broodstock and larval nutrition, larval husbandry and culture conditions, and juvenile growout practices are critical to the continued growth and profitability of clownfish aquaculture.

Despite the availability of literature on the embryonic development of *A. ocellaris* (Madhu et al., 2012; Soman et al., 2021; Yasir and Qin, 2007), a notable gap in replicated empirical data exists for early larval digestive development and physiology for *A. ocellaris*. Larval digestive ontogeny data will help elucidate appropriate feeding and weaning protocols that best promote larval growth and survival while streamlining the production process. At hatching, marine larvae usually rely on a rudimentary, undifferentiated digestive tract with low levels of pancreatic digestive enzymes (Faulk et al., 2007). At first feeding, many species of marine larvae have a limited mouth gape and limited ability to digest complex nutrients, which often restricts them to feeding upon costly live feeds that are small and highly digestible (Faulk et al., 2007; Holt, 2003; Rønnestad et al., 2007). Further into larval development, many species will develop a stomach that allows for the acidic proteolysis of more complex proteins, such as those found in inert microdiets (Rønnestad et al., 2013). Determining key digestive milestones within the larval period allows for the identification of timepoints that would be most effective for weaning from live feeds to an inert microdiet. Streamlining the larval production process of *A. ocellaris* will allow for increases in cost efficiency and lead to more standardized rearing protocols for both the aquaculture industry and eco/evo/devo research laboratories.

This study is the first to describe the morphological development of the digestive tract and digestive enzyme ontogeny of larval *A. ocellaris*. In addition, morphological developmental milestones, growth, and changes in mouth gape height are described. Together, these data can

89 be used to design and standardize *A. ocellaris* culture protocols that optimize larval nutrition,
90 which can help maximize larval growth, survival, and quality (Cahu et al., 2003; Izquierdo, 1996;
91 Lee et al., 2018).
92
93 **2. Methods**
94 All methods were approved under the University of Florida's Institutional Animal Care
95 and Use Committee (IACUC study #202011169). In a 16 – day trial, the larval development,
96 digestive enzyme ontogeny, and digestive tract morphology of *A. ocellaris* was examined.
97 Fertilized nests (n = 4; 340 – 835 eggs) were collected from broodstock pairs of wild-type *A.*
98 *ocellaris* 24 hours prior to hatching and placed in separate 50 L circular tanks attached to a
99 recirculating aquaculture system featuring a moving bed biofilter, 150W UV sterilizer, and a
100 series of filter bags (250 μm, 50 μm, and 10 μm). This system was housed in a climate-
101 controlled room with air temperature maintained at 28 ± 0.5 °C with a 16L:8D photoperiod.
102 Water quality parameters including temperature, dissolved oxygen (DO), pH, NH_3, NO_2^-, salinity,
103 and alkalinity were monitored once weekly. Nests were incubated at 26 °C with gentle aeration
104 until hatching. Mean water quality parameters were as follows: 26.17 ± 0.68 °C temperature,
105 7.96 ± 0.09 pH, 5.48 ± 0.21 mg/L DO, 31.9 ± 1.59 mg/L salinity, 0 mg/L NH_3^-, 0.049 ± 0.066 mg/L
106 NO_2^-, and 218.79 ± 19.37 mg/L $CaCO_3$, and 227 ± 16.27 lux.
107 At one day post-hatch (DPH), water flow was set to five tank turnovers per day and
108 rotifers, *Brachionus plicatilis,* were added twice daily at a density of 10 rotifers/mL. Rotifer
109 cultures were fed daily with RotiGrow® Plus (Reed Mariculture, Campbell, CA, USA) and
110 enriched with Algamac 3050 (Aquafauna Bio-Marine, Hawthorne, CA, USA) prior to adding to

111 larval tanks according to the manufacturer's instructions. Live microalgae, *Tisochrysis lutea,* was
112 added twice daily at a density of 150,000 cells/mL to darken larval culture water. *Artemia*
113 (*Artemia franciscana*) nauplii (instar I-II) were introduced at 5 DPH at a density of 0.05
114 nauplii/mL twice daily and co-fed with rotifers until 8 DPH. From 8 DPH until 15 DPH, *Artemia*
115 nauplii (instar I-II) were fed twice daily at a density of 0.25 nauplii/mL.
116 Larvae were sampled daily for developmental characterization and digestive enzyme
117 quantification before feeding from 0 – 15 DPH. At each sampling timepoint, three to nine larvae
118 were removed from each tank, euthanized with an overdose of buffered MS – 222, and
119 photographed with a Jenoptik ProgRes® C5 microscope camera to evaluate length (mm), mouth
120 gape height (μm), and morphological development. Two to six larvae from each tank were
121 rinsed in reagent-grade water, blotted dry, and distributed equally among two 1.5 mL
122 microcentrifuge tubes, and stored at -80 °C until digestive enzyme analysis. The remaining
123 larvae were pooled and placed in 10 % neutral buffered formalin for histological processing.
124 Total notochord length (TL; n = 18.65 $\pm$ 11.26), upper jaw length, and lower jaw length
125 were digitally measured using a Sedgewick Rafter cell and ImageJ. Mouth gape (n = 11 $\pm$ 2) was
126 calculated using the below equation (Wittenrich et al., 2007)**:**

127 $$Mouth\ Ga \quad (\quad) = \sqrt{(UJL)^2 + (LJL)^2}$$

128 where UJL = upper jaw length and LJL = lower jaw length. To visualize the development
129 of the digestive tract, samples were processed in paraffin and serially sectioned longitudinally
130 to visualize the length of the digestive tract. Alcian Blue (AB) and Periodic Acid Schiff (PAS)
131 stains were used to visualize the general development of digestive organs and the presence of
132 acidic and neutral mucopolysaccharides, which help identify the development of functional

gastric glands (Lipscomb et al., 2020). Larvae were assessed microscopically for developmental milestones including mouth opening, swim bladder inflation, pigmentation, flexion, and metamorphosis.

Trypsin, lipase, and pepsin assays were conducted via spectrophotometric microplate assays adapted from Lipscomb et al. (2020; 2022) and Faulk et al. (2007). Briefly, larval samples were thawed on ice homogenized in either 400 µl of homogenization buffer (20 mM Tris-HCl, 1 mM EDTA, 10 mM $CaCl_2$, 7.5 pH) for pancreatic enzyme assays or 400 µl of reagent-grade deionized water for the acid protease assay. Samples were homogenized with a motorized micropestle and centrifuged at 1700*G for 10 minutes at 4 °C. To quantify lipase activity, aliquots of 10 µl of sample supernatant, homogenization buffer (negative control), or lipase standard (positive control; 10 µg/mL) were pipetted in triplicate into a 96-well plate kept on ice. Aliquots of 200 µl of the substrate (0.5 M Tris-HCl, 6 mM sodium taurocholate, 1 M NaCl, 7.4 pH + 2.38 mg 4-nitrophenyl n-Caproate (4-NPC) in 100 µl ethanol) were rapidly pipetted into each well using a multichannel pipette. The plate was rapidly transferred to the microplate reader and the absorbance at 400 nm was measured every 45 seconds for 30 minutes at 30 °C. Lipase activity (U) was calculated as the micromoles of 4-NPC hydrolyzed per minute per larvae (Lipscomb et al., 2020; Lipscomb et al., 2022). To quantify trypsin activity, aliquots of 20 µl of sample supernatant, homogenization buffer (negative control), or trypsin standard (15 µg/mL; positive control) were pipetted into a 96 – well plate in triplicate. Aliquots of 100 µl of substrate (50 mM Tris-acetate, 20 mM $CaCl_2$, pH 8.2 + 4.35 mg *N*α-benzoyl-DL-arginine *p*-nitroanilide (BAPNA), 100 µl DMSO) were rapidly pipetted into each well using a multichannel pipette. Trypsin activity (U) was calculated as the micromoles of *p*-nitroanilide liberated per minute per

155 larvae (Lipscomb et al., 2020; Lipscomb et al., 2022). To measure acid protease activity, 100 µl
156 aliquots of sample supernatant were transferred to new microcentrifuge tubes. Substrate (2%
157 w/v bovine hemoglobin in 60 mM HCl) was added to each sample tube in 500 µl aliquots and
158 samples were incubated at 37 °C for 20 minutes. The reaction was quenched with the addition
159 of 1 mL of 5% Trichloroacetic acid (TCA). Sample blanks were made by adding 1 mL of 5% TCA
160 before the addition of hemoglobin. Samples and sample blanks were centrifuged at 1700*G for
161 10 minutes, transferred to a 96 – well plate in duplicate 100 µl aliquots, and absorbance was
162 read at 280 nm. Acid protease activity (U) was calculated as micromoles of tyrosine liberated
163 per minute per larvae (Lipscomb et al., 2020).
164 Digestive enzyme activities were visualized using a second order polynomial non-linear
165 regression. Total length and mouth gape were analyzed with a simple linear regression.
166 Regressions were conducted in Prism© (Version 9.3.1). To characterize the timing of notochord
167 flexion, the percentage of larvae in the pre-flexion, flexion, and post-flexion stages was
168 determined. Each stage was defined as follows: pre-flexion was characterized by a straight
169 notochord; flexion occurred when the notochord was upturned and fin rays were in the process
170 of forming; post-flexion occurred when the caudal fin rays were fully formed and the hypural
171 plates were clearly defined (Blanco et al., 2019; Miller et al., 2009). Histological sections for
172 each sampling timepoint ($n = 5 \pm 3$) were analyzed for morphological changes and
173 developments in the buccal cavity, esophagus, stomach, intestine, and rectum. The timing of
174 the development of a functional stomach indicated by the presence of gastric glands and
175 secretion of neutral mucopolysaccharides was of particular interest.
176 **3. Results**

177 3.1 Larval development

178 Newly hatched *A. ocellaris* larvae (n = 35) measured 4.21 ± 0.147 mm (TL) and grew to
179 11.06 ± 1.26 mm (TL) by 15 DPH (n = 9; Figure 1-A). Clownfish larvae had a mouth gape height
180 of 353 ± 35 μm at hatching (n = 35) and their mouth gape grew to 787 ± 2.69 μm by 15 DPH (n
181 = 9; Figure 1-B). Both larval growth (Figure 1-A) and gape height growth (Figure 1-B) followed
182 linear patterns (R^2 = 0.9860 and R^2 = 0.8922), respectively. Eye pigmentation and mouth
183 opening were also observed at 0 DPH (Figure 2). Histological sections (n = 9) showed that at
184 hatching, the gut of *A. ocellaris* was coiled and differentiated into the esophagus, stomach
185 anlage, intestine, and rectum with the yolk reserves and oil globule still present (Figure 3-A).
186 Swim bladder inflation began as early as 0 DPH (n = 5; Figure 3-B). At 1 DPH, yolk and oil globule
187 were reduced, but still present and liver tissue began to grow in the place of the reduced yolk
188 (n = 5; Figure 3-C). Exogenous feeding began at 1 DPH and endogenous yolk reserves were
189 completely depleted by 3 DPH (n = 7). Notochord flexion began as early as 1 DPH (n = 36;
190 27.27%), with 100% of sampled larvae undergoing flexion at 4 DPH (n = 33; Table 1). By 8 DPH,
191 100% of sampled larvae had completed flexion (n = 13; Table 1). More distinct differentiation of
192 the gut occurred by 6 DPH, with the formation of a stomach and increased digestive surface
193 area (Figure 3-D). Metamorphosis began at 9 DPH, indicated by the development of the
194 anterior white band, with subsequent development of the median band between 9 and 12 DPH.
195 Larval settlement began at 11 DPH, indicated by a marked change in swimming behavior and
196 association with structure and the benthos. The development of the caudal peduncle band
197 began after metamorphosis and settlement at 12 DPH. The gut morphology of a 15 DPH
198 juvenile can be seen in Figure 3-E, with further increases in digestive surface area.

199 3.2 Digestive Enzyme Analysis

200 Acid protease (0.678 ± 1.12 U/fish), lipase (152.42 ± 49.93 U/fish), and trypsin activities
201 (39.78 ± 20.25 U/fish) were detectable 24 hours before hatching (Figure 4). Acid protease
202 activity remained low (≤ 2.17 U/fish) until 10 DPH (5.14 U/fish), after which activity gradually
203 increased to 10.60 U/fish by 15 DPH (Figure 4-A). Lipase activity increased gradually throughout
204 the study reaching 42,888.74 U/fish by 15 DPH (Figure 4-B). Trypsin activity was low until 7 DPH
205 (1,429.08 U/fish), after which activity increased to 4,317.57 U/fish at 15 DPH (Figure 4-C).

206 3.3 Histological Analysis

207 *3.3.1 Buccopharyngeal Cavity and Esophagus*

208 At 0 DPH, the buccopharyngeal cavity was characterized by infrequent pharyngeal
209 dentition (n = 7). The esophagus was lined by a cuboidal epithelial layer (n = 10) and the
210 proximal end was characterized by a few PAS-positive goblet cells (n = 9; Figure 5-A). By 3 DPH,
211 flame cells were observed in the proximal buccopharyngeal cavity (n = 8; Figure 5-B). At 6 DPH,
212 the proximal esophagus was lined by a stratified squamous epithelium with more frequent
213 pharyngeal dentition dispersed throughout the epithelium (n = 5; Figure 5-C). The proximal
214 esophagus showed proliferation of PAS-positive goblet cells (n = 5; Figure 5-C). Few PAS-
215 positive goblet cells were observed in the buccopharyngeal cavity at 6 DPH (n = 5; Figure 5-C).
216 At 13 DPH, PAS-positive goblet cells were more frequently dispersed throughout the epithelium
217 of the buccopharyngeal cavity (Figure 5-D). At 15 DPH, goblet cells in the buccal cavity
218 proliferated and flame cells were located frequently throughout the epithelium (Figure 5-E).
219 The esophagus was surrounded by thick walls of smooth and striated muscle (Figure 5-E).

220 *3.3.2 Stomach*

221 Gastric glands were first observed at 6 DPH (n = 3). They were few in number, and the
222 stomach mucosal epithelium had not yet secreted neutral mucins, as indicated by the absence
223 of PAS-positive staining (Figure 6-A). The anterior stomach mucosal epithelium was lined by a
224 cuboidal cell layer, while the posterior stomach mucosa was transitioning into columnar
225 epithelium (n = 3; Figure 6-A). At 7 DPH, the stomach epithelium was stained PAS-positive and
226 by 9 DPH, gastric glands had proliferated, and the mucosa was characterized by columnar
227 epithelial cells (n = 2; Figure 6-B). The size of the stomach and number of gastric glands had
228 increased significantly by 15 DPH and epithelial goblet cells were stained PAS-positive (n = 3;
229 Figure 6-C). Gastric glands were located almost entirely in the anterior portion of the stomach
230 (Figure 6-C).
231 *3.3.3 Intestine*
232 At 0 and 1 DPH, the intestinal mucosa was lined with columnar epithelial cells with
233 basally located nuclei and a visible brush border (n = 5; Figure 7-A). Supranuclear vacuoles were
234 not yet present in the mucosa at 1 DPH. By 6 DPH, digestive surface area had increased with the
235 proliferation of intestinal and rectal rugae (n = 3; Figure 7-B). Supranuclear vacuoles were
236 numerous and located throughout the intestine, with a concentration of vacuoles in the
237 posterior portion of the intestine (Figure 7-B). By 13 DPH, AB-positive goblet cells were
238 dispersed periodically throughout the intestinal mucosa and were present in higher numbers in
239 the rectal mucosa (n = 2; Figure 7-C). At 15 DPH, similar patterns were seen including an
240 increase in complexity, and proliferation of intestinal rugae and supranuclear vacuoles (n = 3;
241 Figure 7-D).
242

4. Discussion

This study is the first to examine the ontogeny of the digestive tract of *A. ocellaris* using enzymatic assays and histology. The morphological development of *A. ocellaris* in this study was similar to the morphological development of conspecifics and congeners. At hatching, *A. percula* larvae ranged from 3.79 – 4.2 mm in length (Gordon and Hecht, 2002; Madhu et al., 2012; Önal et al., 2008) and the total length of *A. frenatus* larvae at 0 DPH was 4.61 mm (Putra et al., 2012). The mouth gape of newly hatched *A. ocellaris* was reported to be between 170 – 210 μm by Madu et al. (2012), which is approximately 143 – 183 μm smaller than the mouth gape height of 0 DPH *A. ocellaris* reported in this study. This discrepancy may be due to differences in measurement methods as no measurement methods were provided and it was unclear whether the gape height or width was reported by Madhu et al. (2012).

The patterns of digestive enzyme activity determined in this study are consistent with other tropical fish species, although the timing of digestive tract maturation tends to be species-specific. In general, pancreatic enzymes including lipase and trypsin are detectable at mouth opening at low levels and increase significantly with age (Zambonino Infante and Cahu, 2001). The activity of pancreatic enzymes, including lipase and trypsin, tend to increase with age because the mechanism of pancreatic enzyme secretion is not fully mature until later in the larval period (Zambonino Infante and Cahu, 2001). The increase of these enzymes during later larval stages also coincides with increased intestinal folding and the maturation of the intestine, indicated by the transition from intracellular digestion to extracellular digestion (Zambonino Infante and Cahu, 2001). These patterns have been seen in the current study, where pancreatic enzyme activities increased steadily later in development, coinciding with increased intestinal

folding (Figure 7B and C). Other studies have reported similar patterns involving tropical fish species including *Lutjanus guttatus* (Moguel-Hernández et al., 2014), *Paramisgurnus dabryanus* (Zhang et al., 2015), and *Gymnocorymbus ternetzi* (Lipscomb et al., 2020). Acid protease activities may not be detectable from hatching and start to increase once gastric glands are formed and functional (Zambonino Infante and Cahu, 2001). In the present study, low levels of acid protease activity were detected prior to gastric gland formation. However, this phenomenon is not unique and is most likely due to the nonspecific nature of the acid protease assay, which can detect other acid enzymes in a whole-body larval homogenate. Martínez-Lagos et al. (2014) found a similar pattern in the larval development of the leopard grouper (*Mycteroperca rosacea*) where acid protease activity was detected much earlier in development than expected, which the authors attributed to the presence of other acid enzymes such as cathepsins that are distributed throughout many different tissues.

Digestive tract morphology of *A. ocellaris* was similar to that of *A. percula* at hatching where the gut was coiled and differentiated into the esophagus, stomach anlage, intestine, and rectum, and the oil globule and yolk sac was prominent (Önal et al., 2008). Many other closely-related damselfish species including *A. melanopus, A. percula, A. frenatus, A. nigripes,* and *Premnas biaculeatus* exhibit an open mouth at hatching (Table 2), mirroring the development of *A. ocellaris* in this study. Yolk absorption and the replacement of the yolk and oil globule by the liver by 3 DPH was reported for *A. percula* (Gordon and Hecht, 2002) *and A. melanopus* (Green and McCormick, 2001). The remainder of digestive development was similar to Gordon and Hecht (2002) including the proliferation of goblet cells in the esophagus by 9 DPH, the

286 increase in number of gastric glands after 6 DPH, and the increase in number and size of
287 supranuclear vacuoles in the intestine later in the larval period (Gordon and Hecht, 2002).
288 The timing of notochord flexion in this study was similar to that found by Roux et al.
289 (2019) where notochord flexion occurred between 2 and 8 DPH in *A. ocellaris* larvae. Reported
290 timings of metamorphosis and settlement of *Amphiprion* clownfishes have ranged from as early
291 as 9 DPH to as late as 25 DPH (Ghosh and Kumar, 2015; Gordon and Hecht, 2002; Madhu et al.,
292 2012). Madhu et al. (2012) reported metamorphosis for *A. ocellaris* to occur between 15 – 17
293 DPH and settlement between 17 – 20 DPH, while Ghosh and Kumar (2015) reported
294 metamorphosis to occur from 25 DPH onwards. Gordon and Hecht (2002) reported
295 metamorphosis of *A. percula* to occur at 9 DPH, where the stomach becomes fully functional
296 and extracellular digestion, indicated by supranuclear vacuoles in the intestine, occurs.
297 The discrepancies surrounding the timing of metamorphosis may be attributed to
298 varying definitions of metamorphosis and certain culture conditions. The former studies used
299 solely morphometric features, namely pigmentation, to indicate metamorphosis. Traditionally,
300 metamorphosis is indicated by the transition of the larvae from an intracellular mode of
301 digestion to an extracellular mode of digestion, which is indicated by the development of
302 gastric digestion (in gastric species) and final maturation of the brush border in the intestine
303 (Rønnestad et al., 2013). In the present study, metamorphosis, which was indicated by both
304 digestive tract maturation and white band formation, began at 9 DPH.
305 White band formation in *A. ocellaris* has been reported to start between 9 – 15 DPH
306 (Ghosh and Chakrabarti, 2015; Madhu et al., 2006; Roux et al., 2019), which is consistent with
307 the results of this study. However, the caudal peduncle band formation has been reported to

start anywhere from 17 DPH to 60 DPH (Madhu et al., 2012; Roux et al., 2019), where this study found the caudal band first developing as early as 12 DPH. The timing of white band formation is largely attributed to the quality of nutrition provided during the larval period. Larval fish are highly dependent on an adequate exogenous supply of highly unsaturated fatty acids (HUFAs) for proper growth and survival. Olivotto et al. (2011) found that *A. ocellaris* larvae offered HUFA-enriched rotifers had significantly higher growth and survival and upregulated gene expression of growth factors (IGFI and IGFII) compared to larvae offered unenriched rotifers. The discrepancy of white band formation on the caudal peduncle may be attributed to differences in larval nutrition between the studies, where either unenriched rotifers (Madhu et al., 2012) or rotifers enriched with *Nannochloropsis* sp. (Roux et al., 2019) were used compared to rotifers enriched with Algamac 3050 used in the present study. Unenriched rotifers or rotifers fed on a monoalgal diet are known to be deficient or unbalanced in HUFAs (Conceição et al., 2010). The use of an enrichment, such as Algamac 3050, can significantly improve the HUFA profiles, including EPA, DHA, and ARA. The improvement of HUFA nutrition through enrichment in this study may have influenced juvenile *A. ocellaris* to form the white caudal band earlier than in other studies.

Culture temperature can significantly impact larval growth, development, and physiology (Ye et al., 2011). While the timing of developmental milestones for *A. ocellaris* were similar to those of *A. percula* found by Gordon and Hecht (2002), these milestones differed from those found by Önal et al. (2002) for *A. percula*. Önal et al. (2002) reported that yolk absorption occurred later at 3 – 5 DPH compared to at 3 DPH reported in the present study. They also reported gastric gland development in *A. percula* at 11 DPH, compared to 5 – 7 DPH

by Gordon and Hecht (2002) and 6 DPH in the present study. These discrepancies in digestive development could be attributed to differences in culture parameters, with temperature being the most notable (Önal et al., 2008). The culture temperature used by Gordon and Hecht (2002) was the same as this study (26°C), which may explain similar timing of gastric gland development contrasted with observations by Önal et al. (2008), where the culture temperature was 24 – 25 °C. Temperature was found to be a significant factor in the larval duration, growth rate, and survival of *A. clarkii* larvae (Ye et al., 2011). Expectedly, a 23°C culture temperature yielded significantly lower growth and survival and a significantly longer larval duration compared to larvae cultured at 29°C (Ye et al., 2011).

Data on key developmental milestones and the corresponding culture temperatures for eight damselfish species are summarized in Table 2. A small number of studies had culture temperatures approximately 1 – 2 °C higher than the present study where yolk absorption occurred by 1 DPH for *A. melanopus, A. frenatus,* and *P. biaculeatus*. Although larval development is relatively plastic given environmental temperature, developmental timepoints for different larval damselfish species also appears to be species-specific. Outside of the genus *Amphiprion,* damselfishes in the genus *Dascyllus* tend to have a shorter incubation period and longer pelagic larval duration (Thresher, 1984). Anzeer et al. (2019) reported that *D. carneus* larvae cultured at 27 – 29 °C underwent flexion between 11 – 15 DPH and settled at 30 DPH, which is over twice the larval duration of *A. ocellaris* reported in the current study. In contrast, a single species of damselfish, *Acanthochromis polyacanthus*, has an extended 15 – 17 day incubation period, undergoes flexion at 10 days after fertilization (DAF), and does not have a pelagic larval stage (Kavanagh, 2000).

352 The development of the digestive tract is key to understanding the types of feeds that
353 larval fish can digest at certain timepoints. In early larval stages, the absence a functional
354 stomach may decrease the digestibility of more complex proteins due to the lack of acidic
355 hydrolysis (Rønnestad et al., 2007). Until digestive tract maturation, larvae must rely upon
356 endocytosis and intracellular digestion by enterocytes, which can limit the efficiency of
357 digestion, especially if large, complex molecules are present (Rønnestad et al., 2007). It is
358 common practice to wean larval fish from live feeds to inert microdiets as early as possible
359 during the aquaculture process to increase production and economic efficiency. These inert
360 microdiets contain more complex polypeptides compared to live feeds, which often contain
361 short peptides and free amino acids that are more easily digested by a larval fish. Studies have
362 utilized digestive enzyme ontogeny and digestive tract morphology to indicate the appropriate
363 timing of weaning larval fish from live feeds to a microdiet. Chen et al. (2021) found that the
364 stomach of *Pseudochromis fridmani* developed between 32 and 36 DPH and that weaning time
365 had a significant effect on larval growth and pigmentation. Larvae that were weaned before the
366 development of a functional stomach showed significantly lower growth and pigmentation
367 compared to larvae weaned after the development of a stomach (Chen et al., 2021). Thompson
368 et al. (2019) found that pigfish larvae had significantly increased survival when weaned at 32
369 DPH after stomach formation compared to just days earlier in the larval period. However,
370 weaning success tends to be species-specific. Lipscomb et al. (2020) found that larval
371 *Gymnocorymbus ternetzi* could be successfully weaned from *Artemia* nauplii to a microdiet at
372 13 DPH, which occurred prior to the development of a functional stomach at 22 DPH. Although
373 gastric glands were first observed at 6 DPH in *A. ocellaris* larvae, full functionality of the

stomach did not occur until 7 DPH, indicated by the secretion of neutral mucins by the stomach mucosa to protect against degradation by hydrochloric acid (Lipscomb, 2020). This indicates that *A. ocellaris* may be able to be fully transitioned from live feeds to a microdiet as early as 7 DPH.

Larval fish are usually classified as either altricial or precocial, which is dependent on the development of the digestive system. Precocial larvae will develop a functional stomach by first feeding while altricial larvae develop a functional stomach at metamorphosis (Rønnestad et al., 2013). These characteristics would classify *A. ocellaris* as altricial because this species does not have a functional stomach at first feeding. However, they are considerably more developed than many other altricial larvae such as Pacific blue tang (*Paracanthurus hepatus*), melanurus wrasse (*Halichoeres melanurus*), or pigfish (*Orthopristis chrysoptera*) that have a rudimentary, undifferentiated straight-tube digestive tract, non-functional eyes, and no mouth at hatching (DiMaggio et al., 2012; DiMaggio et al., 2017; Groover et al., 2021). *A. ocellaris* has a coiled, differentiated digestive tract, functional eyes, and a mouth with a large mouth gape at hatching, therefore they do not have to undergo major organogenesis during the larval period (Önal et al., 2008). Also, *A. ocellaris* larvae may be able to be weaned onto microdiets as early as 7 DPH, at the onset of stomach functionality. Additional studies will need to be conducted to determine the ideal weaning period and diet type(s) that best promotes larval growth and survival.

In conclusion, *A. ocellaris* are considerably well-developed at hatching and develop a mature digestive tract at 7 DPH with subsequent metamorphosis starting at 9 DPH and settlement at 11 DPH. The results from this study provide a more detailed understanding of the

A. ocellaris larval period to not only improve larval culture protocols, but to also move towards standardized rearing practices. Standardized rearing practices will have implications for *A. ocellaris* production for both aquaculture and as a model organism for evolutionary and developmental research.

Table 1. Progress of larval flexion from 0 to 8 DPH represented by percentage of larvae in each stage. N represents sample size for each timepoint.

DPH	Pre-flexion (%)	Undergoing flexion (%)	Post-flexion (%)	N
0	100.00	0.00	0.00	36
1	72.73	27.27	0.00	33
2	11.76	88.24	0.00	34
3	5.88	94.12	0.00	34
4	0.00	100.00	0.00	33
5	0.00	82.35	17.65	17
6	0.00	80.95	19.05	21
7	0.00	23.81	76.19	21
8	0.00	0.00	100.00	13

414 Table 2. Comparative developmental data of eight damselfish species with associated rearing
415 temperature (DPH – days post hatch; DAF – days post fertilization). Data synthesized in
416 this table were derived from peer review literature with similar damselfish species. In
417 cases where developmental data were not explicitly stated, experimental results
418 and/or histology were interpreted to acquire salient data presented below.

Species	Rearing Temperature (°C)	Mouth Open	Yolk Absorbed	Flexion	Stomach differentiation	Metamorphosis	Settlement	Reference
Amphiprion ocellaris	26	0 DPH	3 DPH	3 – 7 DPH	6 DPH	9 DPH	11 DPH	Present study
Amphiprion melanopus	28	0 DPH	3 DPH	0 – 3 DPH	3 DPH	N/A	8 DPH	Green and McCormick, 2001
Amphiprion percula	24 – 25	0 DPH	3-5 DPH	N/A	11 DPH	N/A	N/A	Önal et al., 2008
Amphiprion percula	26	0 DPH	3 DPH	N/A	5 DPH	9 DPH	N/A	Gordon and Hecht, 2002
Amphiprion frenatus	28 – 29	0 DPH	1 DPH	2 – 5 DPH	14 DPH	N/A	N/A	Putra et al., 2012
Amphiprion nigripes	26	0 DPH	1 DPH	4 – 9 DPH	N/A	15 DPH	N/A	Kumar et al., 2012
Premnas biaculeatus	28 – 30	0 DPH	1 DPH	N/A	N/A	12 DPH	N/A	Roy et al., 2014
Dascyllus carneus	27 – 29	2 DPH	3 DPH	11 – 15 DPH	N/A	N/A	30 DPH	Anzeer et al., 2019
Dascyllus trimaculatus	27 – 31	2 DPH	N/A	N/A	N/A	35 – 40 DPH	N/A	Gopakumar et al., 2009
Acanthochromis polyacanthus	27 – 28	0 DPH	2 – 3 DPH	10 DAF	N/A	0 DPH	0 DPH	Kavanagh, 2000

419

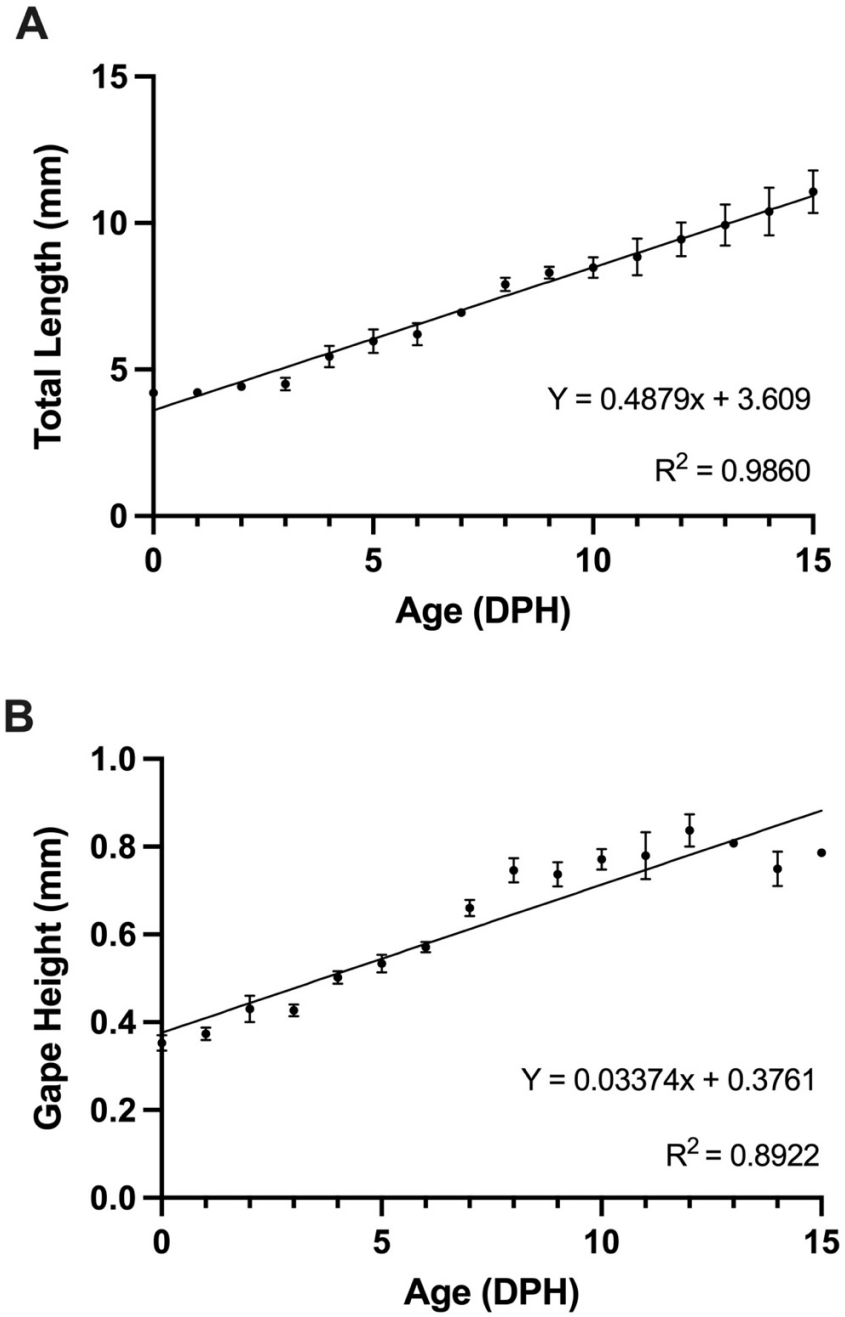

420

421 Figure 1. Growth curve (A; n = 18.65 ± 11.26) and mouth gape growth curve (B; n = 11 ± 2) for
422 *A. ocellaris* from 0 to 15 DPH. Values for larval growth (A) are either notochord length (<
423 5 DPH) or total length (≥ 5 DPH). Error bars represent ± standard error.

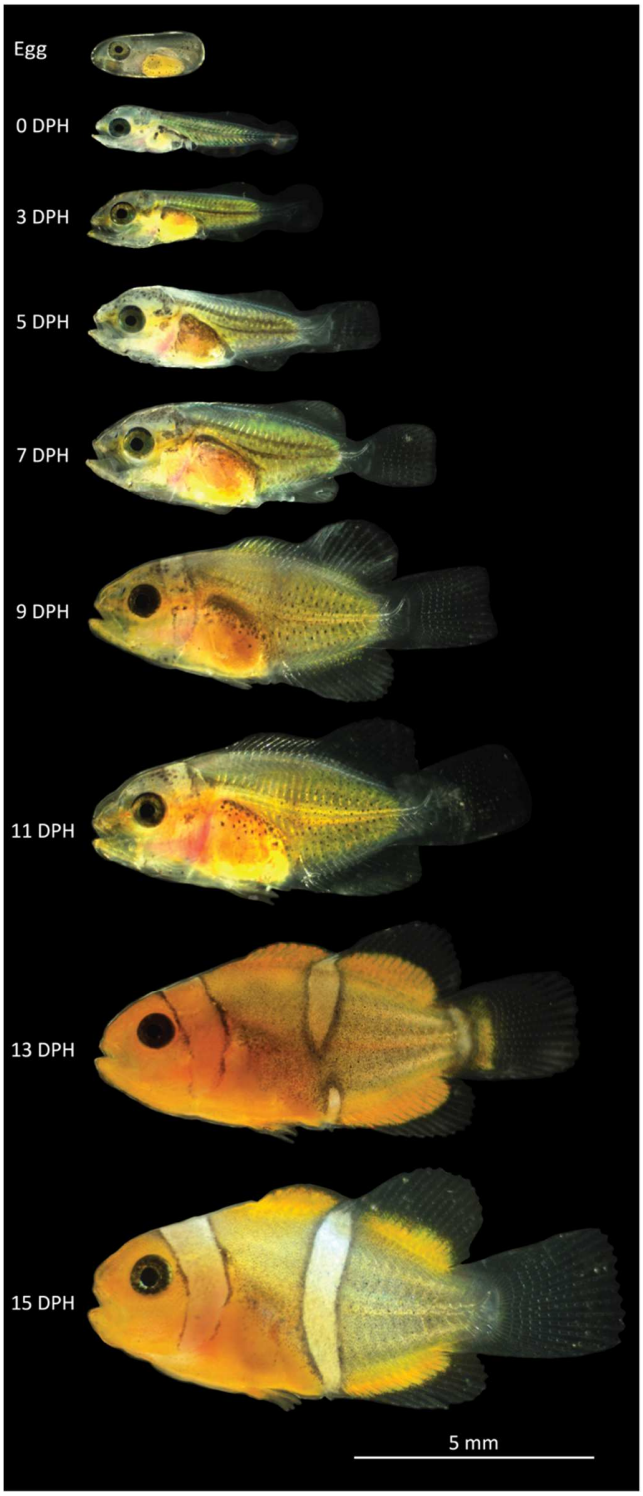

424

425 Figure 2. Morphological development of *A. ocellaris* from 24 hours before hatching (egg) to 15
426 DPH.

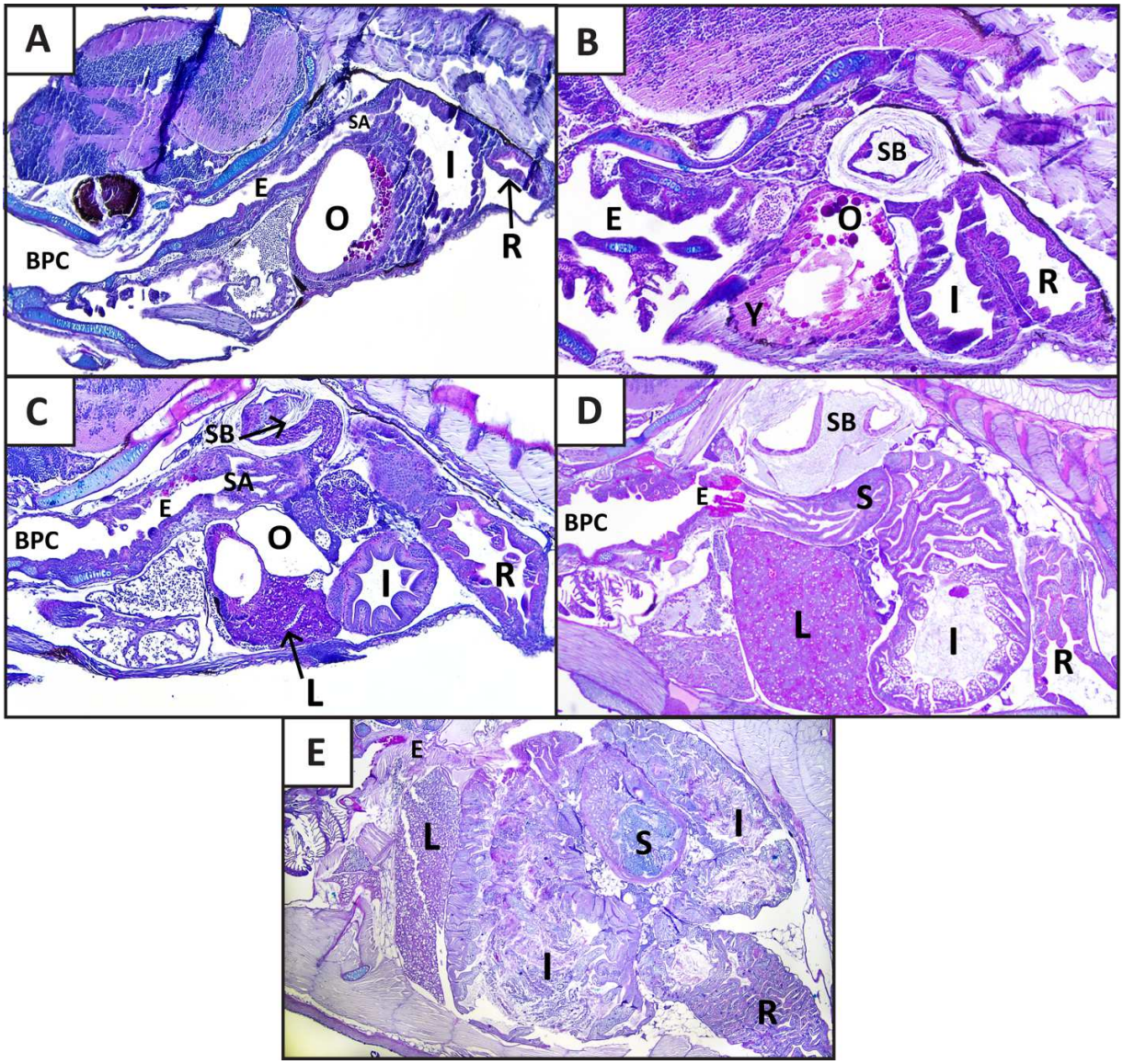

Figure 3. Photomicrographs (AB+PAS) of *A. ocellaris* digestive tract at A & B) 0 DPH (100x), C) 1 DPH (100x), D) 6 DPH (40X), and E) 15 DPH (40X). Buccopharyngeal cavity (BPC), esophagus (E), stomach anlage (SA), swim bladder (SB), stomach (S), oil globule (O), yolk (Y), liver (L), intestine (I), rectum (R).

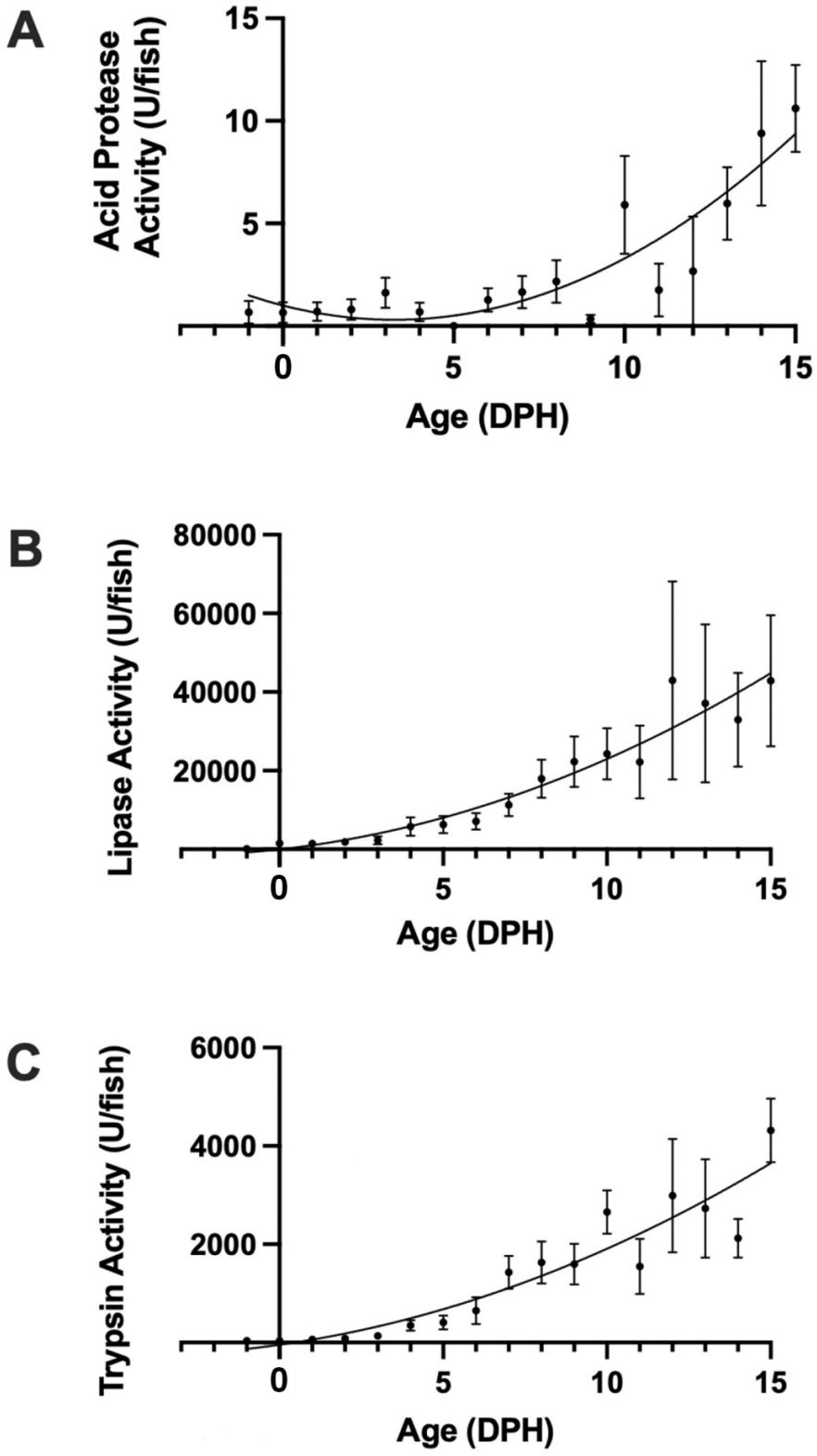
A
Acid Protease Activity (U/fish)
15
10
5
0
5
10
15
Age (DPH)
B
Lipase Activity (U/fish)
80000
60000
40000
20000
0
5
10
15
Age (DPH)
C
Trypsin Activity (U/fish)
6000
4000
2000
0
5
10
15
Age (DPH)

433

Figure 4. Mean digestive enzyme activity (A – Acid Protease, B – Lipase, C – Trypsin; ± SE) of larval *A. ocellaris* from 24 hours before hatching to 15 DPH (n = 4 from 0 - 10 DPH; n = 3 from 11 - 15 DPH). Trendlines were fitted with a second order polynomial nonlinear regression to visualize data trend.

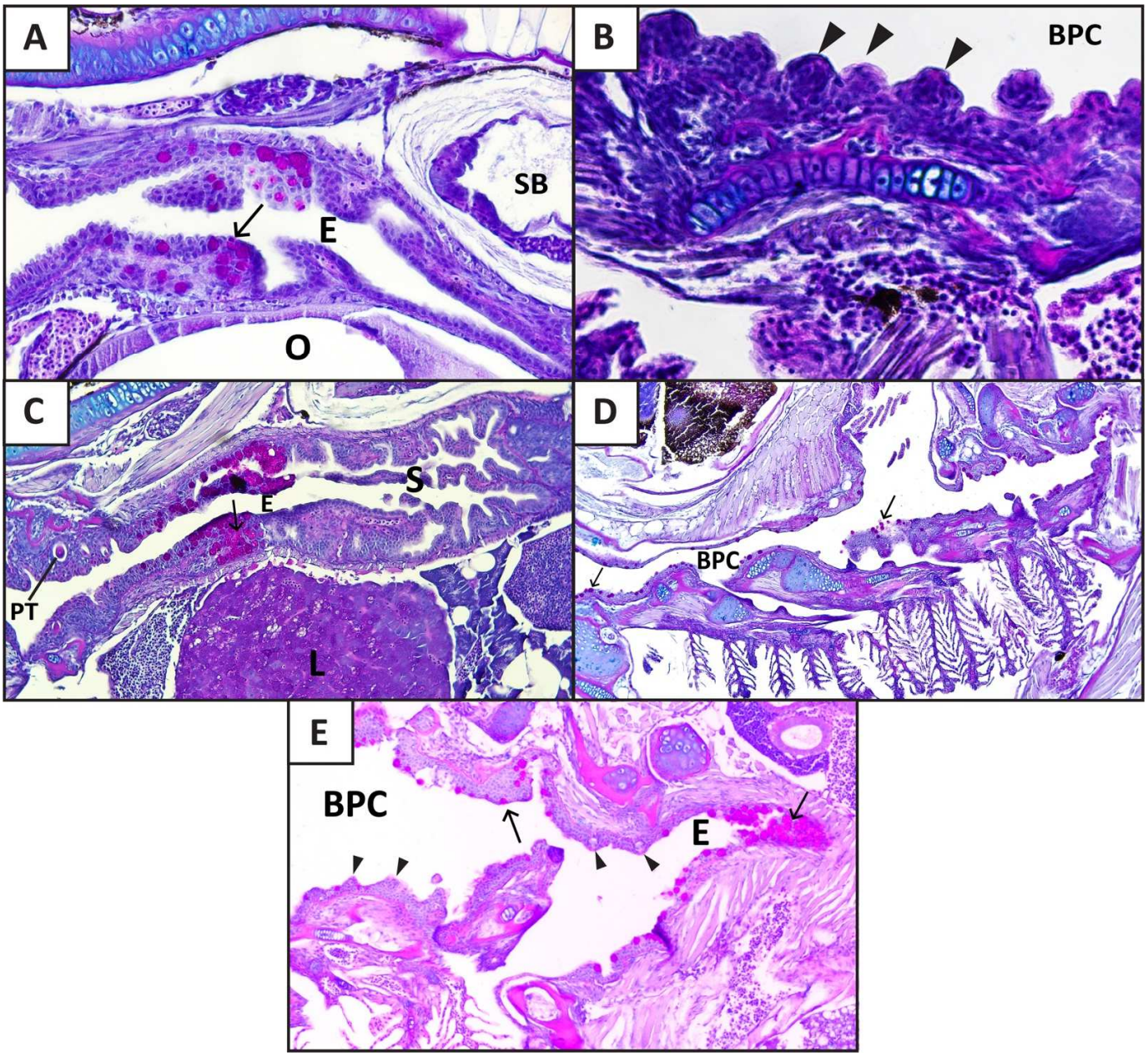

Figure 5. Photomicrographs (AB+PAS) of *A. ocellaris* buccopharyngeal cavity and esophagus at A) 0 DPH (400X), B) 3 DPH (400X), C) 6 DPH (200X), D) 13 DPH (100X), and E) 15 DPH (200X). Buccopharyngeal cavity (BPC), esophagus (E), oil globule (O), pharyngeal teeth (PT), stomach (S), liver (L); swim bladder (SB). Arrows indicate goblet cells. Arrow heads indicate flame cells.

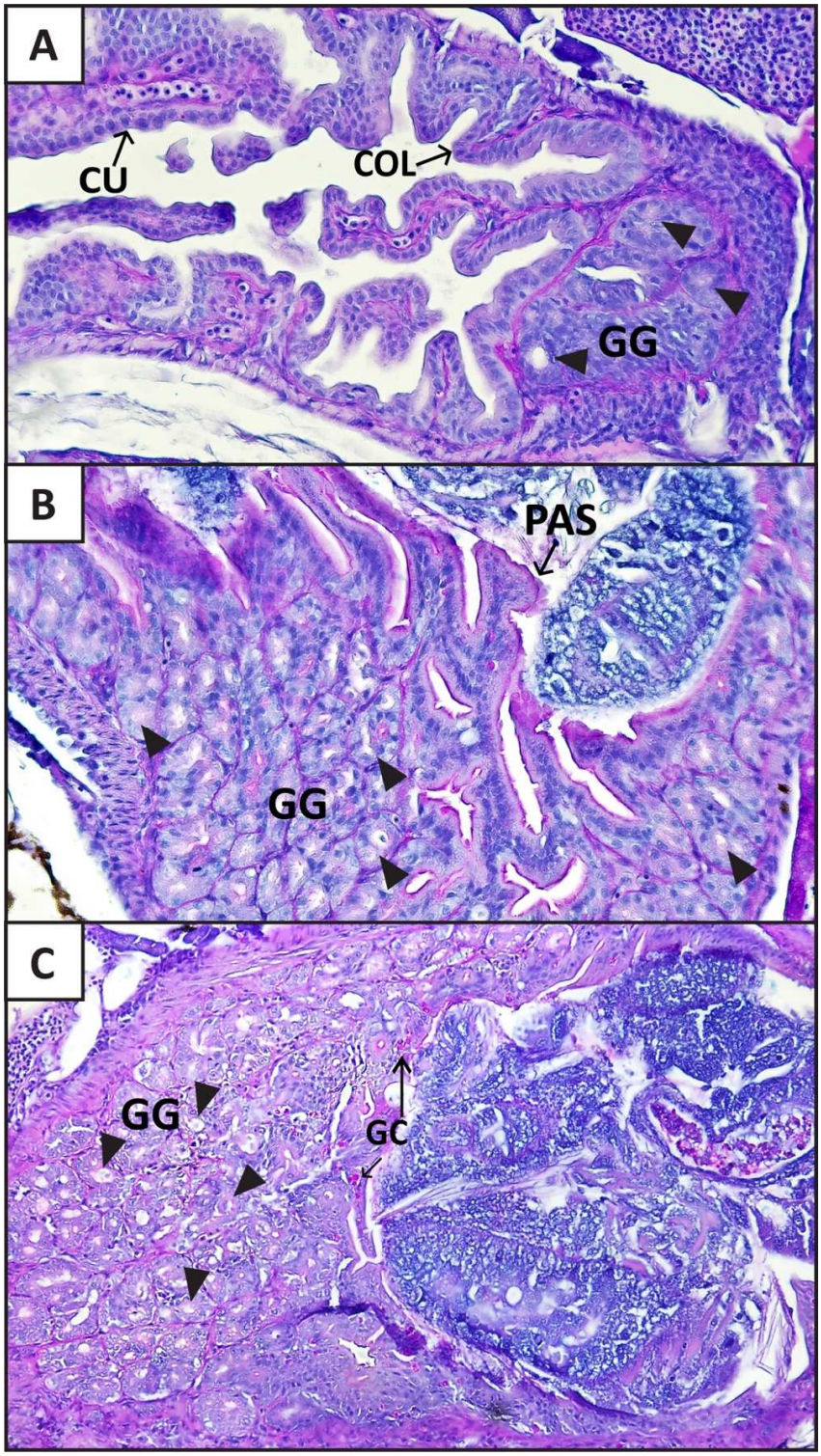

Figure 6. Photomicrographs (AB+PAS) of *A. ocellaris* stomach at A) 6 DPH (400X), B) 9 DPH (400X), and C) 15 DPH (200X). Cuboidal epithelium (CU); columnar epithelium (COL); gastric glands (GG); PAS (Periodic Acid-Schiff positive stain); goblet cells (GC). Arrow heads indicate gastric glands.

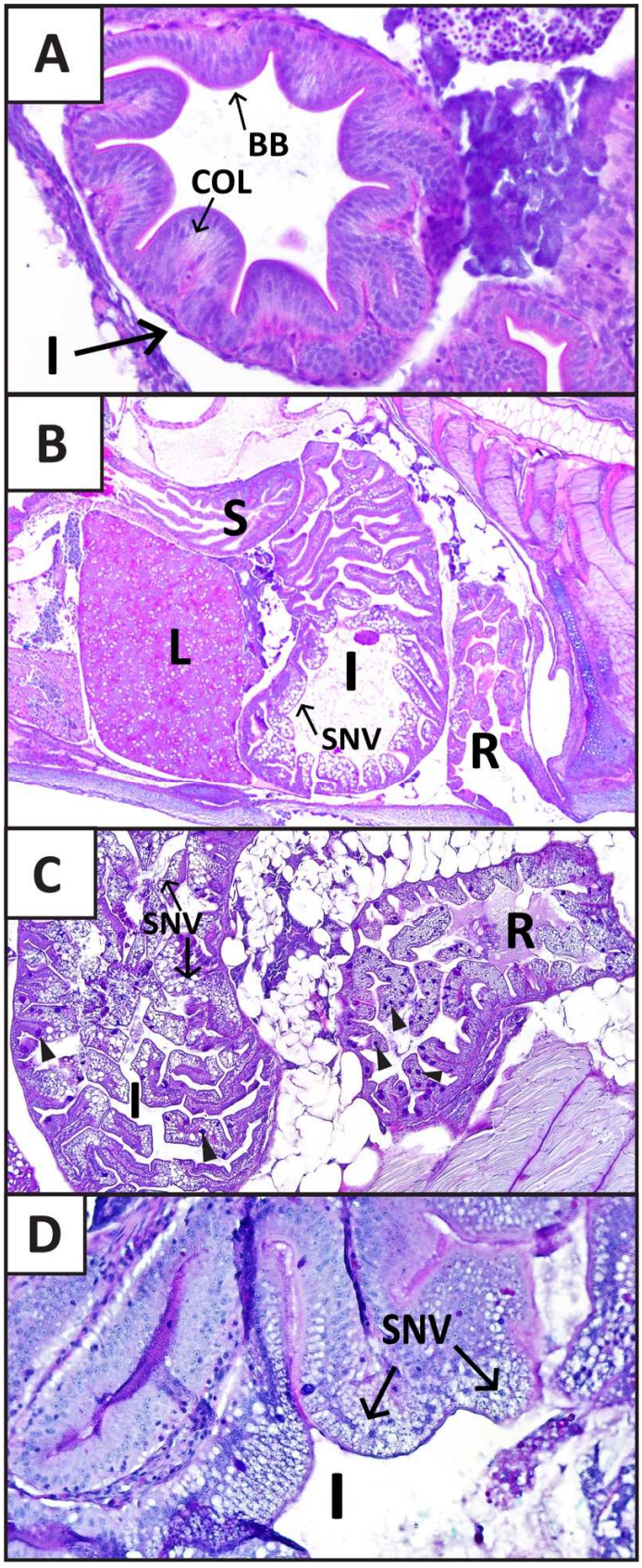

452

Figure 7. Photomicrographs (AB+PAS) of *A. ocellaris* intestine at A) 1 DPH (400X), B) 6 DPH (100X), C) 13 DPH (100X), and D) 15 DPH (400X). Intestine (I), stomach (S), liver (L), columnar epithelium (COL); brush border (BB); supranuclear vacuoles (SNV); rectum (R). Arrow heads indicate goblet cells.

5. Acknowledgements

This work was supported in part by Rising Tide Conservation and the SeaWorld Conservation Fund. We thank Dr. Roy Yanong and Dr. Taylor Lipscomb for their histological expertise. A special thanks to Instant Ocean, Spectrum Brands, Oceans, Reefs, & Aquariums (ORA), and FishEye Aquaculture for donation of materials.

6. References

Ajith Kumar, T. T. and Balasubramanian, T. (2009). Broodstock development, spawning and larval rearing of the false clown fish, Amphiprion ocellaris in captivity using estuarine water. *Curr. Sci.* **97**, 1483–1486.

Anzeer, F. M., Aneesh, K. S., Abraham, M. V., Darsana, S., Santhosh, B., Anil, M. K., Gopalakrishnan, A., Udayakumar, A., Kingsly, H. J., Unnikrishnan, C., et al. (2019). Breeding, early development and larval rearing of cloudy damsel, Dascyllus carneus Fischer, 1885. *Aquaculture* **505**, 374–385.

Blanco, E., Reglero, P., Hernández de Rojas, A., Ortega, A., de la Gándara, F. and Folkvord, A. (2019). The effect of nutritional condition by two nucleic acid derived indices on the growth to post-flexion of Atlantic bluefin tuna and Atlantic bonito larvae. *J. Exp. Mar. Bio. Ecol.* **519**, 151182.

Cahu, C., Infante, J. Z. and Takeuchi, T. (2003). Nutritional components affecting skeletal development in fish larvae. *Aquaculture* **227**, 245–258.

Chen, J. Y., Zeng, C. and Cobcroft, J. M. (2021). Digestive system ontogeny and the effects of

478 weaning time on larval survival, growth and pigmentation development of orchid
479 dottyback Pseudochromis fridmani. *Aquaculture* **549**, 737737.
480 **Conceição, L. E. C., Yúfera, M., Makridis, P., Morais, S. and Dinis, M. T.** (2010). Live feeds for
481 early stages of fish rearing. *Aquac. Res.* **41**, 613–640.
482 **DiMaggio, M. A., Broach, J. S., Ohs, C. L. and Grabe, S. W.** (2012). Captive volitional spawning
483 and larval rearing of Pigfish. *N. Am. J. Aquac.* **75**, 109–113.
484 **DiMaggio, M. A., Cassiano, E. J., Barden, K. P., Ramee, S. W., Ohs, C. L. and Watson, C. A.**
485 (2017). First Record of Captive Larval Culture and Metamorphosis of the Pacific Blue Tang,
486 Paracanthurus hepatus. *J. World Aquac. Soc.* **48**, 393–401.
487 **Faulk, C. K., Benninghoff, A. D. and Holt, G. J.** (2007). Ontogeny of the gastrointestinal tract
488 and selected digestive enzymes in cobia Rachycentron canadum (L.). *J. Fish Biol.* **70**, 567–
489 583.
490 **Ghosh, S. K. and Chakrabarti, P.** (2015). Histological and histochemical characterization on
491 stomach of Mystus cavasius (Hamilton), Oreochromis niloticus (Linnaeus) and Gudusia
492 chapra (Hamilton): Comparative study. *J. Basic Appl. Zool.* **70**, 16–24.
493 **Ghosh, S. and Kumar, T.** (2015). Band transformation secrets of Anemonefish Amphiprion
494 ocellaris. *Indian J. Geo-Marine Sci.* **44**, 902–904.
495 **Gopakumar, G., Ignatius, B., Santhosi, I. and Ramamoorthy, N.** (2009). Controlled Breeding
496 and Larval Rearing Techniques of Marine Ornamental Fishes. *Asian Fish. Sci.* **22**, 797–804.
497 **Gordon, A. K. and Hecht, T.** (2002). Histological studies on the development of the digestive
498 system of the clownfish Amphiprion percula and the time of weaning. *J. Appl. Ichthyol.* **18**,
499 113–117.

Green, B. S. and McCormick, M. I. (2001). Ontogeny of the digestive and feeding systems in the anemonefish Amphiprion melanopus. *Environ. Biol. Fishes* **61**, 73–83.

Groover, E. M., Alo, M. M., Ramee, S. W., Lipscomb, T. N., Degidio, J. M. L. A. and DiMaggio, M. A. (2021). Development of early larviculture protocols for the melanurus wrasse Halichoeres melanurus. *Aquaculture* **530**, 735682.

Hoff, F. H. (1996). *Conditioning,spawning,and rearing of fish with emphasis on marine clownfish*. (ed. Moe, M.), Lichtenbert, J.), and Johnson, D.) Dade City, FL: Aquaculture Consultants, Inc.

Holt, G. (2003). Research on culturing the early life stages of marine ornamental species. In *Marine Ornamental Species: collection, culture and conservation* (ed. Cato, J.) and Brown, C. L.), pp. 251–254. John Wiley & Sons, Ltd.

Izquierdo, M. S. (1996). Essential fatty acid requirements of cultured marine fish larvae. *Aquac. Nutr.* **2**, 183–191.

Kavanagh, K. D. (2000). Larval brooding in the marine damselfish Acanthochromis polyacanthus (Pomacentridae) is correlated with highly divergent morphology, ontogeny and life-history traits. *Bull. Mar. Sci.* **66**, 321–337.

Kumar, T. T. A., Gopi, M., Dhaneesh, K. V., Vinoth, R., Ghosh, S., Balasubramanian, T. and Shunmugaraj, T. (2012). Hatchery production of the clownfish Amphiprion nigripes at Agatti island, Lakshadweep, India. *J. Environ. Biol.* **33**, 623–628.

Lee, I. S., Ohs, C. L., Broach, J. S., DiMaggio, M. A. and Watson, C. A. (2018). Determining live prey preferences of larval ornamental marine fish utilizing fluorescent microspheres. *Aquaculture* **490**, 125–135.

Lipscomb, T. (2020). Using Larval Digestive System Ontogeny to Inform Larviculture Protocols in Freshwater Ornamental Fishes.

Lipscomb, T. N., Yanong, R. P., Ramee, S. W. and DiMaggio, M. A. (2020). Histological, histochemical and biochemical characterization of larval digestive system ontogeny in black tetra Gymnocorymbus ternetzi to inform aquaculture weaning protocols. *Aquaculture* **520**, 734957.

Lipscomb, T. N., Durland Donahou, A., Yanong, R. P., Boldt, N. C. and DiMaggio, M. A. (2022). Investigations into Early Larval Feeding Practices for the Tiger Barb Puntigrus tetrazona. *N. Am. J. Aquac.* **84**, 53–65.

LiveAquaria.com (2022). All Captive-Bred Fish.

Madhu, K., Madhu, R., Krishnan, L., Sasidharan, C. S., Venugopalan, K. M. and CMFRI, K. (2006). Spawning and larval rearing of Amphiprion ocellaris under captive condition. *Mar Fish Inf Serv Tech Ext Ser.* **188**, 1–5.

Madhu, R., Madhu, K. and Retheesh, T. (2012). Life history pathways in false clown Amphiprion ocellaris Cuvier, 1830: A journey from egg to adult under captive condition. *J. Mar. Biol. Assoc. India* **54**, 77–90.

Martínez-Lagos, R., Tovar-Ramírez, D., Gracia-López, V. and Lazo, J. P. (2014). Changes in digestive enzyme activities during larval development of leopard grouper (Mycteroperca rosacea). *Fish Physiol. Biochem.* **40**, 773–785.

Miller, B., Kendall, A. W. and Miller, B. (2009). *Early Life History of Marine Fishes*. Berkeley, UNITED STATES: University of California Press.

Moguel-Hernández, I., Peña, R., Nolasco-Soria, H., Dumas, S. and Zavala-Leal, I. (2014).

544 Development of digestive enzyme activity in spotted rose snapper, Lutjanus guttatus
545 (Steindachner, 1869) larvae. *Fish Physiol. Biochem.* **40**, 839–848.
546 **Önal, U., Langdon, C. and Çelik, I.** (2008). Ontogeny of the digestive tract of larval percula
547 clownfish, Amphiprion percula (Lacépède 1802): A histological perspective. *Aquac. Res.* **39**,
548 1077–1086.
549 **Palmtag, M.** (2017). The marine ornamental species trade. In *Marine Ornamental Species*
550 *Aquaculture* (ed. Calado, R.), Olivotto, I.), Oliver, P.), and Holt, J.), pp. 3–14. John Wiley &
551 Sons, Ltd.
552 **Penning, M., Reid, G. M., Koldewey, H., Dick, G., Andrews, B., Arai, K., Garratt, P., Gendron,**
553 **S., Lange, J., Tanner, K., et al.** (2009). *Turning the Tide: A Global Aquarium Strategy for*
554 *Conservation and Sustainability. World Association of Zoos and Aquariums*.
555 **Putra, D. F., Abol-Munafi, A. B., Muchlisin, Z. A. and Chen, J. C.** (2012). Preliminary studies on
556 morphology and digestive tract development of tomato clownfish, Amphiprion frenatus
557 under captive condition. *AACL Bioflux* **5**, 29–35.
558 **Raghavan, R., Dahanukar, N., Tlusty, M. F., Rhyne, A. L., Krishna Kumar, K., Molur, S. and**
559 **Rosser, A. M.** (2013). Uncovering an obscure trade: Threatened freshwater fishes and the
560 aquarium pet markets. *Biol. Conserv.* **164**, 158–169.
561 **Rhyne, A. L., Tlusty, M. F., Schofield, P. J., Kaufman, L., Morris, J. A. and Bruckner, A. W.**
562 (2012). Revealing the appetite of the marine aquarium fish trade: The volume and
563 biodiversity of fish imported into the united states. *PLoS One* **7**,.
564 **Rhyne, A. L., Tlusty, M. F., Szczebak, J. T. and Holmberg, R. J.** (2017). Expanding our
565 understanding of the trade in marine aquarium animals. *PeerJ* **2017**,.

Rønnestad, I., Kamisaka, Y., Conceição, L. E. C., Morais, S. and Tonheim, S. K. (2007). Digestive physiology of marine fish larvae: Hormonal control and processing capacity for proteins, peptides and amino acids. *Aquaculture* **268**, 82–97.

Rønnestad, I., Yúfera, M., Ueberschär, B., Ribeiro, L., Sæle, Ø. and Boglione, C. (2013). Feeding behaviour and digestive physiology in larval fish: Current knowledge, and gaps and bottlenecks in research. *Rev. Aquac.* **5**,.

Roux, N., Salis, P., Lambert, A., Logeux, V., Soulat, O., Romans, P., Frédérich, B., Lecchini, D. and Laudet, V. (2019). Staging and normal table of postembryonic development of the clownfish (Amphiprion ocellaris). *Dev. Dyn.* **248**, 545–568.

Roux, N., Salis, P., Lee, S. H., Besseau, L. and Laudet, V. (2020). Anemonefish, a model for Eco-Evo-Devo. *Evodevo* **11**, 1–11.

Roux, N., Logeux, V., Trouillard, N., Pillot, R., Magré, K., Salis, P., Lecchini, D., Besseau, L., Laudet, V. and Romans, P. (2021). A star is born again: Methods for larval rearing of an emerging model organism, the False clownfish Amphiprion ocellaris. *J. Exp. Zool. Part B Mol. Dev. Evol.* **336**, 376–385.

Roy, S. D., Ray, B. C., Sarma, K. and George, G. (2014). CAPTIVE BREEDING AND LARVAL REARING OF MAROON SPINY DAMSEL FISH , Premnas biaculeatus (BLOCH , 1790) Brood stock collection Embryogenesis study. **19**, 78–87.

Soman, M., Chadha, N. K., Madhu, K., Madhu, R., Sawant, P. B. and Francis, B. (2021). Optimization of temperature improves embryonic development and hatching efficiency of false clown fish, Amphiprion ocellaris Cuvier, 1830 under captive condition. *Aquaculture* **536**, 736417.

588 **Thompson, K. L., Faulk, C. K. and Fuiman, L. A.** (2019). Applying the ontogeny of digestive
589 enzyme activity to guide early weaning of pigfish, Orthopristis chrysoptera (L.). *Aquac. Res.*
590 **50**, 1404–1410.
591 **Thresher, R. E.** (1984). Reproduction in Reef Fishes.p. 399. Neptune City, N.J.: T.F.H Publication,
592 Inc Ltd.
593 **Whittington, R. J. and Chong, R.** (2007). Global trade in ornamental fish from an Australian
594 perspective: The case for revised import risk analysis and management strategies. *Prev.*
595 *Vet. Med.* **81**, 92–116.
596 **Wittenrich, M. L., Turingan, R. G. and Creswell, R. L. R.** (2007). Spawning, early development
597 and first feeding in the gobiid fish Priolepis nocturna. *Aquaculture* **270**, 132–141.
598 **Yasir, I. and Qin, J. G.** (2007). Embryology and early ontogeny of an anemonefish Amphiprion
599 ocellaris. *J. Mar. Biol. Assoc. United Kingdom* **87**, 1025–1033.
600 **Ye, L., Yang, S.-Y., Zhu, X.-M., Liu, M., Lin, J.-Y. and Wu, K.-C.** (2011). Effects of temperature on
601 survival, development, growth and feeding of larvae of Yellowtail clownfish Amphiprion
602 clarkii (Pisces: Perciformes). *Acta Ecol. Sin.* **31**, 241–245.
603 **Zambonino Infante, J. L. and Cahu, C. L.** (2001). Ontogeny of the gastrointestinal tract of
604 marine fish larvae. *Comp. Biochem. Physiol. - C Toxicol. Pharmacol.* **130**, 477–487.
605 **Zhang, Y. L., Wu, Q. W., Hu, W. H., Wang, F., Zhao, Z. B., He, H., Shao, W. H. and Fan, Q. X.**
606 (2015). Changes in digestive enzyme activities during larval development of Chinese loach
607 Paramisgurnus dabryanus (Dabry de Thiersant, 1872). *Fish Physiol. Biochem.* **41**, 1577–
608 1585.
609